New Journal of Physics
The open-access journal for physics

Magnetism and quantum phase transitions in spin-1/2 attractive fermions with polarization

J-S He[1], A Foerster[2], X W Guan[3] and M T Batchelor[3,4,5]

[1] Department of Mathematics, Ningbo University, Ningbo, 315211 Zhejiang, People's Republic of China
[2] Instituto de Fisica da UFRGS, Avenida Bento Goncalves, 9500, Porto Alegre 91501-970, Brasil
[3] Department of Theoretical Physics, Research School of Physics and Engineering, Australian National University, Canberra ACT 0200, Australia
[4] Mathematical Sciences Institute, Australian National University, Canberra ACT 0200, Australia
E-mail: Murray.Batchelor@anu.edu.au

New Journal of Physics **11** (2009) 073009 (17pp)
Received 16 March 2009
Published 3 July 2009
Online at http://www.njp.org/
doi:10.1088/1367-2630/11/7/073009

Abstract. An extensive investigation is given for magnetic properties and phase transitions in one-dimensional (1D) Bethe ansatz integrable spin-1/2 attractive fermions with polarization by means of the dressed energy formalism. An iteration method is presented to derive higher order corrections for the ground-state energy, critical fields and magnetic properties. Numerical solutions of the dressed energy equations confirm that the analytic expressions for these physical quantities and resulting phase diagrams are highly accurate in the weak and strong coupling regimes, capturing the precise nature of magnetic effects and quantum phase transitions in 1D interacting fermions with population imbalance. Moreover, it is shown that the universality class of linear field-dependent behaviour of the magnetization holds throughout the whole attractive regime.

[5] Author to whom any correspondence should be addressed.

Contents

1. Introduction

Bosons and fermions reveal strikingly different quantum statistical effects at low temperatures. Bosons with integer spin undergo Bose–Einstein condensation (BEC), whereas fermions with half-odd-integer spin are not allowed to occupy a single quantum state due to the Pauli exclusion principle. However, fermions with opposite spin states can pair up to produce Bardeen–Cooper–Schrieffer (BCS) pairs to form a Fermi superfluid. Quantum degenerate gases of ultracold atoms open up exciting possibilities for the experimental study of such subtle quantum many-body physics in low dimensions [1]–[4]. In this platform, Feshbach resonance has given rise to a rich avenue for the experimental investigation of relevant problems, such as the crossover from BCS superfluidity to BEC [5], fermionic superfluidity and phase transitions, among others [6]–[8]. Particularly, pairing and superfluidity are attracting further attention from theory and experiment due to the close connection to high-T_c superconductivity and nuclear physics. The study of pairing signature and fermionic superfluidity in interacting fermions has stimulated growing interest in Fermi gases with population imbalance [9]–[12] i.e. systems with different species of fermions [3] as well as multicomponent interacting fermions [13]–[16]. This gives rise to new perspectives to explore subtle quantum phases, such as a breached pairing phase [17] and a nonzero momentum pairing phase of Fulde–Ferrell–Larkin–Ovchinnikov (FFLO) states [18, 19] and colour superfluids [4].

One-dimensional (1D) atomic gases with internal degrees of freedom also provide tunable interacting many-body systems featuring novel magnetic properties and quantum phase transitions [20]–[24]. Although the FFLO state has not been fully confirmed experimentally, investigations of the elusive FFLO state in the 1D interacting Fermi gas with population imbalance are very promising [25]–[35], [38]–[42]. Theoretical predictions for the existence of an FFLO state in the 1D interacting Fermi gas has emerged by a variety of methods including the Bethe ansatz (BA) solution [26], numerical methods [28], [30]–[32], [34, 38, 42] and field theory [35, 43, 44]. A powerful field theory approach [35, 44] was used to describe an FFLO state in the 1D Fermi superliquid with population imbalance. Nevertheless, verification of the FFLO signature of polarized attractive fermions is still lacking via the BA solution. A recent thermodynamic Bethe ansatz (TBA) study of strongly attractive fermions [27] shows that paired and unpaired atoms from two Fermi liquids coupled to each other. The TBA equations indicate that spin wave fluctuations ferromagnetically couple to the unpaired Fermi sea. A full analysis

of magnetic effects and low energy physics of spin-1/2 fermions with polarization in both the weak and strong coupling regimes, as well as a detailed discussion on the universality class of the magnetic behaviour in the whole attractive regime, are desirable in understanding such subtle paired states in 1D interacting fermions with polarization.

In the present paper, we provide an extended investigation of quantum phases and phase transitions for 1D interacting fermions with polarization in the presence of an external field. We analytically and numerically solve the dressed energy equations that describe the equilibrium state at zero temperature. We extend the previous work on this model to derive higher order corrections (up to order $1/|\gamma|^3$) for the ground-state energy, magnetization, critical fields, chemical potentials and the external field–energy transfer relation. The phase diagrams in the weak and strong coupling regimes are obtained in terms of the external field, density and interaction strength. In the strong coupling regime, (i) the bound pairs in the homogeneous system form a singlet ground state when the external field is less than the lower critical value H_{c1}, (ii) a normal Fermi liquid phase without pairing occurs when the external field is greater than the upper critical value H_{c2}, and (iii) for an intermediate range $H_{c1} < H < H_{c2}$, paired and unpaired atoms coexist. However, for weak coupling, a BCS-like pair scattering phase occurs only when the external field $H = 0$, while paired and unpaired fermions coexist when the field is less than a critical field. Significantly, we also show that the universality class of linear field-dependent behaviour of the magnetization remains throughout the whole attractive regime.

The present paper is set out as follows. In section 2, we present the Hamiltonian and discuss the pairing signature for the 1D fermions with population imbalance in the whole attractive regime. In section 3, we present the dressed energy equations obtained from the TBA equations in the limit $T \to 0$. In section 4, we present the magnetic properties for the model in the weak coupling regime. We solve the dressed energy equations in the strong-coupling regime in section 5. The explicit forms of the magnetic properties and the ground-state energy are given in terms of the interaction strength, density and external field. In section 6, we present the full phase diagrams for the whole attractive regime. Section 7 is devoted to concluding remarks and a brief discussion.

2. The model

The Hamiltonian [47, 48] we consider

$$\mathcal{H} = \sum_{j=\downarrow,\uparrow} \int_0^L \phi_j^\dagger(x) \left(-\frac{\hbar^2}{2m} \frac{\mathrm{d}^2}{\mathrm{d}x^2} \right) \phi_j(x) \mathrm{d}x + g_{1\mathrm{D}} \int_0^L \phi_\downarrow^\dagger(x) \phi_\uparrow^\dagger(x) \phi_\uparrow(x) \phi_\downarrow(x) \mathrm{d}x$$
$$- \frac{1}{2} H \int_0^L \left(\phi_\uparrow^\dagger(x) \phi_\uparrow(x) - \phi_\downarrow^\dagger(x) \phi_\downarrow(x) \right) \mathrm{d}x \tag{1}$$

describes N δ-interacting spin-1/2 fermions of mass m constrained by periodic boundary conditions to a line of length L and subject to an external magnetic field H. In this formulation, the field operators $\phi_\downarrow$ and $\phi_\uparrow$ describe fermionic atoms in the respective states $|\uparrow\rangle$ and $|\downarrow\rangle$. The δ-type interaction between fermions with opposite hyperfine states preserves the spin states such that the Zeeman term in the Hamiltonian (1) is a conserved quantity. For convenience, we use units of $\hbar = 2m = 1$ and define $c = m g_{1\mathrm{D}}/\hbar^2$ and a dimensionless interaction strength $\gamma = c/n$ for the physical analysis, where $n = N/L$ is the linear density. The inter-component interaction can be tuned from strongly attractive ($g_{1\mathrm{D}} \to -\infty$) to strongly repulsive ($g_{1\mathrm{D}} \to +\infty$) via

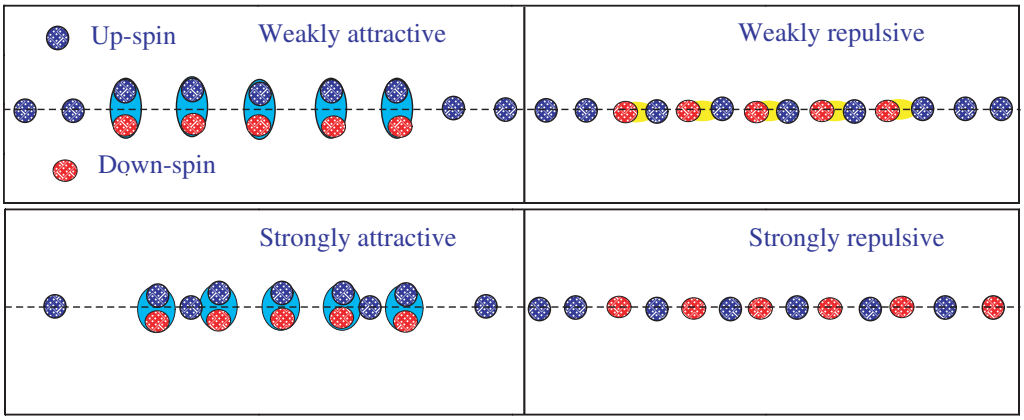

Figure 1. BA root configurations for pairing and depairing in quasimomentum space. For weakly attractive interaction, unpaired roots sit in the out wings due to strong Fermi pressure. For strongly attractive interaction, unpaired roots can penetrate into the central region, occupied by the bound pairs. However, for weakly repulsive interaction the roots with up- and down-spins separate gradually. In the strongly repulsive regime, the model forms an effective Heisenberg spin chain with the antiferromagnetic coupling constant $J \approx -4E_{\rm F}/\gamma$ [52], where $E_{\rm F} = n^2\pi^2/3$ is the Fermi energy.

Feshbach resonance and optical confinement. The interaction is attractive for $g_{1D} < 0$ and repulsive for $g_{1D} > 0$.

The model (1) was solved by Yang [47] and Gaudin [48] in the 1960s and has received renewed interest in connection with ultracold atomic gases [20]–[32], [34, 35], [38]–[42]. The energy eigenspectrum is given by $E = \frac{\hbar^2}{2m}\sum_{j=1}^{N} k_j^2$, where the BA wave numbers $\{k_i\}$ and the rapidities $\{\Lambda_\alpha\}$ for the internal spin degrees of freedom satisfy the BA equations:

$$\exp(\mathrm{i}k_j L) = \prod_{\ell=1}^{M} \frac{k_j - \Lambda_\ell + \mathrm{i}\,c/2}{k_j - \Lambda_\ell - \mathrm{i}\,c/2}, \quad \prod_{\ell=1}^{N} \frac{\Lambda_\alpha - k_\ell + \mathrm{i}\,c/2}{\Lambda_\alpha - k_\ell - \mathrm{i}\,c/2} = -\prod_{\beta=1}^{M} \frac{\Lambda_\alpha - \Lambda_\beta + \mathrm{i}\,c}{\Lambda_\alpha - \Lambda_\beta - \mathrm{i}\,c}. \tag{2}$$

Here $j = 1, \ldots, N$ and $\alpha = 1, \ldots, M$, with M the number of spin-down fermions.

The solutions to the BA equations (2), as depicted in figure 1, provide a clear pairing signature and the ground-state properties of the model. The BA root distributions in the complex plane were studied recently [23, 29]. The ground state for 1D interacting fermions with repulsive interaction has antiferromagnetic ordering [23, 49, 50]. Rather subtle magnetism for the model with repulsive interaction was recently studied [51, 52]. For attractive interaction, fermions with different spin states can form BCS pairs with nonzero centre-of-mass momenta, which might feature FFLO states [26, 28], [30]–[32], [34, 35].

In the weakly attractive regime, the weakly bound Cooper pairs are not stable due to thermal and spin wave fluctuations. The unpaired fermions sit on two outer wings in the quasimomentum space [23, 27] due to the Fermi pressure (see figure 1). The ground state can only have one pair of fermions with opposite spins having a particular quasimomentum k. The paired fermions occupy the central area in the quasimomentum k space. Indeed, we find from the BA equations (2) that in the weak coupling limit, i.e. $L|c| \ll 1$, the imaginary

part of the quasimomenta for a BCS pair is proportional to $\sqrt{|c|/L}$. However, for strongly attractive interaction, i.e. $L|c| \gg 1$, the BCS pair has imaginary part $\pm i\frac{1}{2}|c|$. In this regime, the lowest spin excitation has an energy gap, which is proportional to c^2. For the cross-over regime, i.e. $L|c| \sim 1$, the imaginary part $\pm iy$ is asymptotically determined by the condition $y \tanh(\frac{1}{2}yL) \approx \frac{1}{2}|c|$. For this cross-over regime, the spin gap might be exponentially small. However, it is hard to analytically determine this small energy gap from the BA equations (2). Nevertheless, for the weak coupling regime $L|c| \ll 1$, the bound state has a small binding energy $\epsilon_b = \hbar^2 n|\gamma|/mL$, which has the same order of γ as the interacting energies of pair–pair and pair–unpaired fermions. In this limit, the real parts of the quasimomenta satisfy the Gaudin model-like BA equations [23, 36], which describe BCS pair–pair and pair–unpaired fermion scattering. They form a gapless superconducting phase. Using the above BA root configuration, the ground-state energy per unit length is given by [23]

$$E \approx \frac{\hbar^2 n^3}{2m}\left(-\frac{|\gamma|}{2}(1-P^2)+\frac{\pi^2}{12}+\frac{\pi^2}{4}P^2\right) \tag{3}$$

in terms of the polarization $P = (N-2M)/N$. The first term in equation (3) includes the collective interaction energy (pair–pair and pair–unpaired fermion scattering energy) and the binding energy (internal energy). We see clearly that for large polarization ($P \approx 1$) the small portion of spin-down fermions are likely to experience a mean-field formed by the spin-up medium. This is consistent with the observation of Fermi polarons in an attractive Fermi liquid of ultracold atoms [37].

On the other hand, when the attractive interaction strength is increased, i.e. $L|c| \gg 1$, the bound pairs gradually form hard-core bosons, while the unpaired fermions can penetrate into the central region in the quasimomentum space (see figure 1). The main reason for the unpaired fermions and BCS pairs having overlapping Fermi seas is that in 1D the paired and unpaired fermions have different fractional statistical signatures such that they are allowed to pass into each other in the quasimomentum space. In the thermodynamic limit, i.e. $L \to \infty$, $N \to \infty$ with N/L finite, the binding energy of a pair is $\epsilon_b = \hbar^2 n^2 \gamma^2/(4m)$. The dimensionless interaction strength $\gamma = c/n$ is inversely proportional to the density n. This signature leads to different phase segments in 1D trapped fermions [25]–[27] than the phase separations in 3D trapped interacting fermions, where the Fermi gas has been separated into a uniformly paired inner core surrounded by a shell with the excess of unpaired atoms [6]–[8].

From the ground-state energy for the model with strong attraction and arbitrary polarization [23], we find the finite-size corrections to the energy in the thermodynamic limit to be given by

$$E(L,N) - LE_0^{\infty} \approx -\frac{\pi\hbar C}{6L}(v_b + v_u), \tag{4}$$

where the central charge $C = 1$ and the group velocities for bound pairs v_b and unpaired fermions v_u are

$$\begin{aligned} v_b &\approx \frac{v_F(1-P)}{4}\left(1+\frac{(1-P)}{|\gamma|}+\frac{4P}{|\gamma|}\right), \\ v_u &\approx v_F P\left(1+\frac{4(1-P)}{|\gamma|}\right). \end{aligned} \tag{5}$$

Here the Fermi velocity is $v_F = \hbar\pi n/m$. In the above equation, E_0^∞ is the ground-state energy in the thermodynamic limit

$$E_0^\infty \approx \frac{\hbar^2 n^3}{2m}\left\{-\frac{(1-P)\gamma^2}{4}+\frac{P^3\pi^2}{3}\left(1+\frac{4(1-P)}{|\gamma|}\right)+\frac{\pi^2(1-P)^3}{48}\left(1+\frac{(1-P)}{|\gamma|}+\frac{4P}{|\gamma|}\right)\right\}. \quad (6)$$

The nature of the finite-size corrections indicates that two Fermi liquids couple to each other and have different statistical signatures. The low energy physics is dominated by the charge density fluctuations. The spin wave fluctuations are frozen out. In order to understand the pairing signature and the subtle FFLO states in 1D, one should investigate density distributions, pairing correlations and thermodynamics, which we do here through the TBA formalism. In particular, we shall focus on magnetic properties and quantum phase transitions for the whole attractive regime.

3. TBA

The TBA provides a powerful and elegant way to study the thermal properties of 1D integrable systems. It also provides a convenient formalism to analyse quantum phase transitions and magnetic effects in the presence of external fields at zero temperature [45], [53]–[55]. In the thermodynamic limit, the grand partition function is $Z = \mathrm{tr}(\mathrm{e}^{-\mathcal{H}/T}) = \mathrm{e}^{-\mathrm{G/T}}$, in terms of the Gibbs free energy $G = E - HM^z - \mu n - TS$ and the magnetization H, the chemical potential μ and the entropy S [45], [53]–[55]. The TBA equations for the attractive regime are much more subtle and involved compared with those for the repulsive regime. In general, the equilibrium states satisfy the condition of minimizing the Gibbs free energy G with respect to the particle and hole densities for the charge and spin degrees of freedom that generates the TBA equations (details are given in [53, 55, 56]). At zero temperature, the ground-state properties are determined in terms of the dressed energies for the paired ϵ^{b} and unpaired fermions ϵ^{u} and the function

$$a_m(x) = \frac{1}{2\pi}\frac{m|c|}{(mc/2)^2+x^2} \quad (7)$$

by

$$\begin{aligned}\epsilon^{\mathrm{b}}(\Lambda) &= 2\left(\Lambda^2-\mu-\frac{1}{4}c^2\right)-\int_{-B}^{B}a_2(\Lambda-\Lambda')\epsilon^{\mathrm{b}-}(\Lambda')\mathrm{d}\Lambda'-\int_{-Q}^{Q}a_1(\Lambda-k)\epsilon^{\mathrm{u}-}(k)\mathrm{d}k,\\ \epsilon^{\mathrm{u}}(k) &= \left(k^2-\mu-\frac{1}{2}H\right)-\int_{-B}^{B}a_1(k-\Lambda)\epsilon^{\mathrm{b}-}(\Lambda)\mathrm{d}\Lambda,\end{aligned} \quad (8)$$

which are the dressed energy equations [27, 45, 53] obtained from the TBA equations in the limit $T \to 0$. The superscripts $\pm$ denote the positive and negative parts of the dressed energies, with the negative (positive) part corresponding to occupied (unoccupied) states. The integration boundaries B and Q characterize the Fermi surfaces of the bound pairs and unpaired fermions, respectively.

The Gibbs free energy per unit length at zero temperature is given by

$$G(\mu, H) = \frac{1}{\pi}\int_{-B}^{B}\epsilon^{\mathrm{b}-}(\Lambda)\mathrm{d}\Lambda+\frac{1}{2\pi}\int_{-Q}^{Q}\epsilon^{\mathrm{u}-}(k)\mathrm{d}k. \quad (9)$$

The TBA equations provide a clear configuration for band fillings with respect to the external field H and chemical potential μ. The polarization P varies with respect to the external magnetic field. From the Gibbs free energy we have the relations

$$-\partial G(\mu, H)/\partial\mu = n, \quad -\partial G(\mu, H)/\partial H = nP/2. \tag{10}$$

4. Magnetic properties in the weak coupling regime

For weak coupling $|c| \to 0$ caution needs to be taken in the thermodynamic limit. On solving the discrete BA equations (2) in the regime $L|c| \ll 1$ the imaginary part of the BCS-like pairs tends to $\sqrt{|c|/L}$ [23]. However, the TBA equations [27, 53] usually follow from the root patterns in the thermodynamic limit, i.e. $L, N \to \infty$ with N/L is fixed. Under this limit, we naturally have the BA root patterns $k_j = \Lambda_j \pm \mathrm{i}\frac{1}{2}|c|$ with $j = 1, \ldots, M$ for the charge degree and the string patterns with equally spaced imaginary distribution for spin rapidity $\Lambda^n_{\alpha,j} = \Lambda^{(n)}_\alpha + \mathrm{i}\frac{1}{2}(n+1-2j)c$, with $j = 1, \ldots, n$. Here the number of strings $\alpha = 1, \ldots, N_n$. Λ^n_α is the position of the centre for the length-n string on the real axis in Λ-space. Therefore, in the weak coupling limit, i.e. $|c| \to 0$, the integral BA equations and the TBA equations do not properly described the true solutions to the discrete BA equations (2) unless under the thermodynamic limit conditions. Nevertheless, the discrepancy is minimal, i.e. it is $O(\gamma^2)$.

The BA equations (2) in principle give complete states of the model. However, at finite temperatures, the true physical states become degenerate. The dressed energies in the TBA equations (8) characterize excitation energies above the Fermi surfaces of the bound pairs and unpaired fermions. All physical quantities, for example, free energy, pressure and magnetic properties can be obtained from the TBA equations without deriving the spectral properties of low-lying excitations. In the weak coupling limit, the interaction energy is proportional to $|c|$, which is much less than the kinetic energy. Therefore, in this regime, the exact ground-state energy with leading term of order $|c|$ is precise enough to capture the nature of phase transitions and magnetic ordering.

From the ground-state energy (3) we have the relation between the external field and magnetization

$$H \approx \frac{\hbar^2 n^2}{2m}\left[2\pi^2 m^z + 4|\gamma|m^z\right], \tag{11}$$

where $m^z = M^z/n$ and the magnetization is defined by $M^z = nP/2$. A linear field-dependent behaviour of the magnetization is observed. Figure 2 shows the magnetization versus the field H for different interaction values $|\gamma|$. We observe that the analytic results plotted from (11) are in excellent agreement with the numerical curves evaluated directly from the dressed energy equations (8). We also find that a fully paired ground state only occurs in the absence of the external field. However, for $H \geqslant H_c$ where

$$H_c = n^2[\pi^2 + 2|\gamma|] \tag{12}$$

the fully polarized phase occurs. Paired and unpaired fermions coexist in the intermediate range $0 < H < H_c$. The phase diagram for weak coupling is illustrated in figure 3.

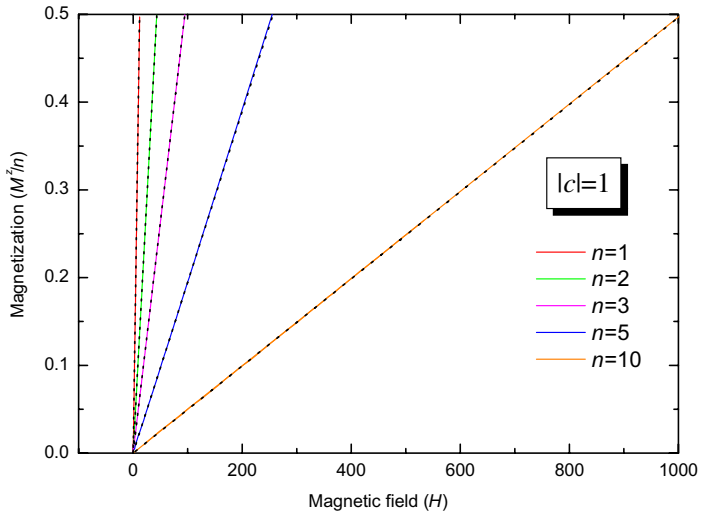

Figure 2. Magnetization M^z/n versus external field H in units $2m = \hbar = 1$ with weak coupling $|c| = 1$ for different densities n. The dashed lines are plotted from the analytic result (11). Excellent agreement between the analytic result and numerical solution of the integral equations (8) (solid lines) is seen.

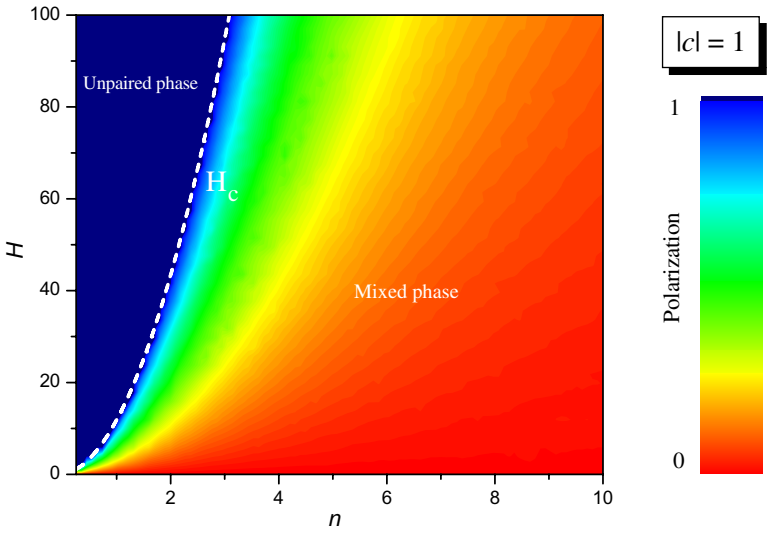

Figure 3. Phase diagram for weak coupling value $|c| = 1$. The dashed line plotted from the analytic result (12) is in excellent agreement with the coloured phases, which are obtained from numerical solutions of the dressed energy equations (8).

5. Solutions to the dressed energy equations

In this section, we solve the dressed energy equations (8) analytically in the strong coupling regime to obtain explicit forms for the critical fields and magnetic properties in terms of the interaction strength γ. We present a systematic way to obtain these physical properties up to order $1/|\gamma|^3$ which gives a very precise phase diagram for finite strong interaction. Here, we note that Iida and Wadati [29] have presented a different method to solve the dressed

energy equations. We have solved the dressed energy equations (8) numerically in the whole attractive regime to compare with the analytic results. Excellent agreement between numerical and analytical results is found.

First consider the ground state $P = 0$. Following the method developed in [27] where the dressed energy equations (8) are asymptotically expanded in terms of $1/|c|$, the ground state dressed energy equation for $P = 0$ is given by

$$\epsilon^{\mathrm{b}}(\Lambda) \approx 2(\Lambda^2 - \bar{\mu}) - \frac{|c|}{\pi}\int_{-B}^{B} \frac{\epsilon^{\mathrm{b}}(\Lambda')}{c^2 + (\Lambda - \Lambda')^2}\mathrm{d}\Lambda' \tag{13}$$

with $\bar{\mu} = \mu + (c^2/4)$. For convenience, we introduce the notation

$$p^{\mathrm{b}} = -\frac{1}{\pi}\int_{-B}^{B} \epsilon^{\mathrm{b}}(\Lambda)\mathrm{d}\Lambda, \tag{14}$$

$$p^{\mathrm{u}} = -\frac{1}{2\pi}\int_{-Q}^{Q} \epsilon^{\mathrm{u}}(k)\mathrm{d}k \tag{15}$$

for the pressure of bound pairs and un-paired fermions. Since the Fermi point B is finite, we can take an expansion with respect to Λ' in the integral in equation (13). By a straightforward calculation, the pressure p^{b} is found to be

$$p^{\mathrm{b}} \approx -\frac{4}{\pi}\left(\frac{B^3}{3} - \bar{\mu}B\right) - \frac{2B}{\pi}\frac{p^{\mathrm{b}}}{|c|} + \frac{128}{45\pi^2|c|^3}(\bar{\mu})^3. \tag{16}$$

We obtained this equation by iteration in terms of p^{b} and $\bar{\mu}$. In such a way, the accuracy of physical quantities can be controlled to powers of $1/|c|$. This provides a systematic way to obtain accurate results from dressed energy equations. It is free from restriction on the integration boundaries B and Q. Furthermore, from equation (16) and the condition $\epsilon^{\mathrm{b}}(\pm B) = 0$, we find

$$B^2 \approx \bar{\mu} - \frac{p^{\mathrm{b}}}{2|c|} + \frac{8}{5\pi|c|^3}(\bar{\mu})^{5/2}. \tag{17}$$

Finally, using the above equations and the relation $\partial p^{\mathrm{b}}/\partial\mu = n$, the pressure per unit length follows as

$$p^{\mathrm{b}} \approx \frac{\hbar^2 n^3}{2m}\frac{\pi^2 n^3}{24}\left(1 + \frac{3}{2|\gamma|} + \frac{3}{2|\gamma|^2} + \frac{1}{4|\gamma|^3}\left(5 - \frac{\pi^2}{3}\right)\right) \tag{18}$$

and the energy per unit length is

$$E_0 \approx \frac{\hbar^2 n^3}{2m}\left\{-\frac{\gamma^2}{4} + \frac{\pi^2}{48}\left[1 + \frac{1}{|\gamma|} + \frac{3}{4|\gamma|^2} + \frac{1}{2|\gamma|^3}\left(1 - \frac{\pi^2}{15}\right)\right]\right\}. \tag{19}$$

The dressed energy equations (8) can also be solved analytically for $0 < P < 1$. Following [27], we define $\tilde{\mu} = \mu + H/2$. We note that the Fermi points Q and B are still finite in the presence of an external field H. Similar to the case $P = 0$, using the conditions $\epsilon^{\mathrm{b}}(\pm B) = 0$ and $\epsilon^{\mathrm{u}}(\pm Q) = 0$, we obtain the relations

$$p^{\mathrm{b}} \approx -\frac{4}{\pi}\left(\frac{B^3}{3} - \bar{\mu}B\right) - \frac{2B}{\pi}\frac{p^{\mathrm{b}}}{|c|} - \frac{8B}{\pi}\frac{p^{\mathrm{u}}}{|c|} + \frac{128\bar{\mu}}{45\pi^2|c|^3} + \frac{64(\bar{\mu})^{3/2}(\tilde{\mu})^{3/2}}{9\pi^2|c|^3} + \frac{64(\bar{\mu})^{1/2}(\tilde{\mu})^{5/2}}{15\pi^2|c|^3}, \tag{20}$$

$$p^{\mathrm{u}} \approx -\frac{Q}{\pi}\left(\frac{Q^2}{3}-\tilde{\mu}\right)-\frac{2Q}{\pi}\frac{p^{\mathrm{b}}}{|c|}+\frac{64(\bar{\mu})^{3/2}(\tilde{\mu})^{3/2}}{9\pi^2|c|^3}+\frac{64(\tilde{\mu})^{1/2}(\bar{\mu})^{5/2}}{15\pi^2|c|^3} \tag{21}$$

and

$$\begin{aligned} B^2 &\approx \bar{\mu}+\frac{p^{\mathrm{b}}}{2|c|}-\frac{2p^{\mathrm{u}}}{|c|}+\frac{4\bar{\mu}^{5/2}}{3\pi|c|^3}+\frac{16\tilde{\mu}^{2/2}\bar{\mu}}{3\pi|c|^3}+\frac{4(\bar{\mu})^{5/2}+16(\tilde{\mu})^{5/2}}{15\pi|c|^3}, \\ Q^2 &\approx \tilde{\mu}-\frac{2p^{\mathrm{b}}}{|c|}+\frac{64(\bar{\mu})^{3/2}\tilde{\mu}}{3\pi|c|^3}+\frac{64(\bar{\mu})^{5/2}}{15\pi|c|^3}. \end{aligned} \tag{22}$$

After eliminating B and Q, we have

$$p^{\mathrm{b}} \approx \frac{8}{3\pi}\left(\bar{\mu}-\frac{p^{\mathrm{b}}+p^{\mathrm{u}}}{2|c|}+\frac{24(\bar{\mu})^{5/2}+16(\tilde{\mu})^{5/2}+80(\tilde{\mu})^{3/2}\bar{\mu}}{15\pi|c|^3}\right)^{3/2}-\frac{160(\bar{\mu})^3+640(\bar{\mu})^{3/2}(\tilde{\mu})^{3/2}}{45\pi^2|c|^3}, \tag{23}$$

$$p^{\mathrm{u}} \approx \frac{2}{3\pi}\left(\tilde{\mu}-\frac{2p^{\mathrm{b}}}{|c|}+\frac{64(\bar{\mu})^{3/2}\tilde{\mu}}{3\pi|c|^3}+\frac{64(\bar{\mu})^{5/2}}{15\pi|c|^3}\right)^{3/2}-\frac{128(\bar{\mu})^{3/2}(\tilde{\mu})^{3/2}}{9\pi|c|^3}. \tag{24}$$

Obviously, the pressures p^{b} and p^{u} are functions of $\bar{\mu}$, $\tilde{\mu}$ and the interaction strength c, i.e. $p^{\mathrm{b}}=p^{\mathrm{b}}(\bar{\mu},\tilde{\mu},|c|)$ and $p^{\mathrm{u}}=p^{\mathrm{u}}(\bar{\mu},\tilde{\mu},|c|)$. Furthermore, taking into account the relations $(\partial p^{\mathrm{b}}/\partial H)+(\partial p^{\mathrm{u}}/\partial H)=P/2$ and $(\partial p^{\mathrm{b}}/\partial\mu)+(\partial p^{\mathrm{u}}/\partial\mu)=n$, after a tedious calculation we find the effective chemical potentials for the pairs $\mu^{\mathrm{b}}=\mu+\epsilon_{\mathrm{b}}/2$ and for the unpaired fermions $\mu^{\mathrm{u}}=\tilde{\mu}=\mu+H/2$. Explicitly,

$$\begin{aligned} \mu^{\mathrm{u}} \approx \frac{\hbar^2n^2\pi^2}{2m}\Bigg\{ & P^2+\frac{(1-P)(49P^2-2P+1)}{12|\gamma|}+\frac{(1-P)^2(93P^2+2P+1)}{8\gamma^2} \\ & -\frac{(1-P)}{240|\gamma|^3}\left[1441\pi^2P^4-7950P^4-324\pi^2P^3+15720P^3-7620P^2\right. \\ & \left.+166\pi^2P^2-120P-4\pi^2P-30+\pi^2\right]\Bigg\}, \end{aligned} \tag{25}$$

$$\begin{aligned} \mu^{\mathrm{b}} \approx \frac{\hbar^2n^2\pi^2}{2m}\Bigg\{ & \frac{(1-P)^2}{16}+\frac{(3P+1)(6P^2-3P+1)}{12|\gamma|}+\frac{(1-P)(5+17P-P^2+491P^3)}{64\gamma^2} \\ & +\frac{1}{240|\gamma|^3}\left[15(1+2P^2)+7470P^3+10\pi^2P^2-180\pi^2P^3\right. \\ & \left.+335\pi^2P^4-420\pi^2P^5-15405P^4-\pi^2+75P+7815P^5\right]\Bigg\}. \end{aligned} \tag{26}$$

These results give rise to a full characterization of two Fermi surfaces. The total chemical potential can be determined from either $\mu^{\mathrm{b}}=\mu+\epsilon_{\mathrm{b}}/2$ or from $\mu^{\mathrm{u}}=\mu+H/2$. The chemical potentials for the fermions with spin-up and spin-down states are determined by $\mu_{\uparrow}=\mu+H/2$

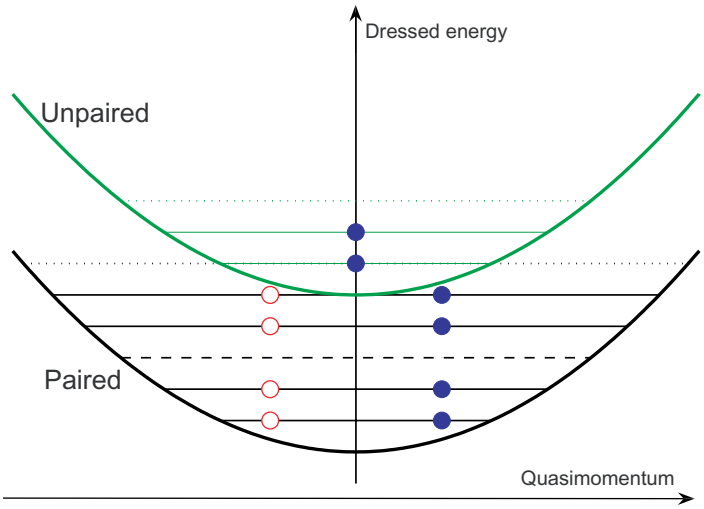

Figure 4. Schematic dressed energy configuration for the gapless phase in the vicinity of H_{c1}.

and $\mu_\downarrow = \mu - H/2$. The energy for the model with arbitrary population imbalances can be obtained from $E/L = \mu n - G + HP/2$, with result

$$\frac{E}{L} \approx \frac{\hbar^2 n^3 \pi^2}{2m}\left\{-\frac{(1-P)\gamma^2}{4}+\frac{\pi^2(1-3P+3P^2+15P^3)}{48}\right.$$
$$+\frac{\pi^2(1-P)(1+P-5P^2+67P^3)}{48|\gamma|}+\frac{\pi^2(1-P)^2(1+5P+3P^2+247P^3)}{64\gamma^2}$$
$$-\frac{\pi^2(1-P)}{1440|\gamma|^3}\left[-15+31125P^4+1861\pi^2P^5-15765P^5-659\pi^2P^4\right.$$
$$\left.\left.+346\pi^2P^3-14\pi^2P^2+\pi^2P+\pi^2-105P-150P^2-15090P^3\right]\right\}. \quad (27)$$

This result provides higher order corrections in terms of the interaction strength γ compared with previous studies [27, 29].

6. Quantum phase transitions

In section 4, we examined magnetic effects and phase transitions for spin-1/2 weakly attractive fermions with polarization. As the attractive interaction strength $|\gamma|$ increases, the bound pairs become stable and form a singlet ground state. The ground-state configuration is characterized by an empty unpaired Fermi sea, whereas the Fermi sea of the bound pairs is filled up to the Fermi surface. The first critical field value H_{c1} diminishes the gap, thus the excitations are gapless. This critical field indicates a phase transition from a singlet ground state into a gapless phase where two Fermi liquids of paired and unpaired fermions couple to each other. These configurations are depicted in figure 4.

Analysis of the dressed energy equations (8) reveals that a fully paired phase with magnetization $M^z = 0$ is stable when the field $H < H_{c1}$, where

$$H_{c1} \approx \frac{\hbar^2 n^2}{2m}\left[\frac{\gamma^2}{2} - \frac{\pi^2}{8}\left(1 - \frac{3}{4|\gamma|^2} - \frac{1}{|\gamma|^3}\right)\right]. \tag{28}$$

In the vicinity of the critical field H_{c1}, the system exhibits a linear field-dependent magnetization

$$M^z \approx \frac{2(H - H_{c1})}{n\pi^2}\left(1 + \frac{2}{|\gamma|} + \frac{11}{2\gamma^2} + \frac{81 - \pi^2}{6|\gamma|^3}\right) \tag{29}$$

with a finite susceptibility

$$\chi \approx \frac{2}{n\pi^2}\left(1 + \frac{2}{|\gamma|} + \frac{11}{2\gamma^2} + \frac{81 - \pi^2}{6|\gamma|^3}\right). \tag{30}$$

This universality class of linear field-dependent magnetization behaviour is also found for the multicomponent Fermi gases with attractive interaction [57]. However, it differs subtly from the case of a Fermi–Bose mixture due to the different statistical signature of a boson and a bound pair of fermions with opposite spin states [52]. For the model under consideration here the magnetic properties in this gapless phase can be exactly described by the external field-magnetization relation

$$\tfrac{1}{2}H = \tfrac{1}{2}\epsilon_b + \mu^u - \mu^b, \tag{31}$$

where μ^u and μ^b are given by (25) and (26) with $P = 2M^z/n = 2m^z$. This relation reveals an important energy transfer relation among the binding energy, the variation of Fermi surfaces and the external field. This relation might provide evidence for the pairing signature in a 1D imbalanced Fermi gas with attractive interaction, i.e. pairs with nonzero centre-of-mass momenta. The lower critical field is reminiscent of the Meissner effect, whereas the upper critical field determined by (31) is reminiscent of a quantum phase transition from superconducting to normal states [58]. Figure 5 shows the magnetization versus external field for different values of the interaction strength γ. Numerical solution of the dressed energy equations (8) shows that the analytic results are highly accurate in the strong and finitely strong coupling regimes.

A similar configuration occurs for the external field exceeding the upper critical field H_{c2}, given by

$$H_{c2} \approx \frac{\hbar^2 n^2}{2m}\left[\frac{\gamma^2}{2} + 2\pi^2\left(1 - \frac{4}{3|\gamma|} + \frac{16\pi^2}{15|\gamma|^3}\right)\right], \tag{32}$$

where a phase transition from the mixed phase into the normal Fermi liquid phase occurs. Figure 6 shows this configuration in the dressed energy language. From the relation (31), we obtain the linear field-dependent magnetization as

$$M^z \approx \frac{n}{2}\left[1 - \frac{H_{c2} - H}{4n^2\pi^2}\left(1 + \frac{4}{|\gamma|} + \frac{12}{\gamma^2} - \frac{16(\pi^2 - 6)}{3|\gamma|^3}\right)\right] \tag{33}$$

with a finite susceptibility

$$\chi \approx \frac{1}{8n\pi^2}\left(1 + \frac{4}{|\gamma|} + \frac{12}{\gamma^2} - \frac{16(\pi^2 - 6)}{3|\gamma|^3}\right). \tag{34}$$

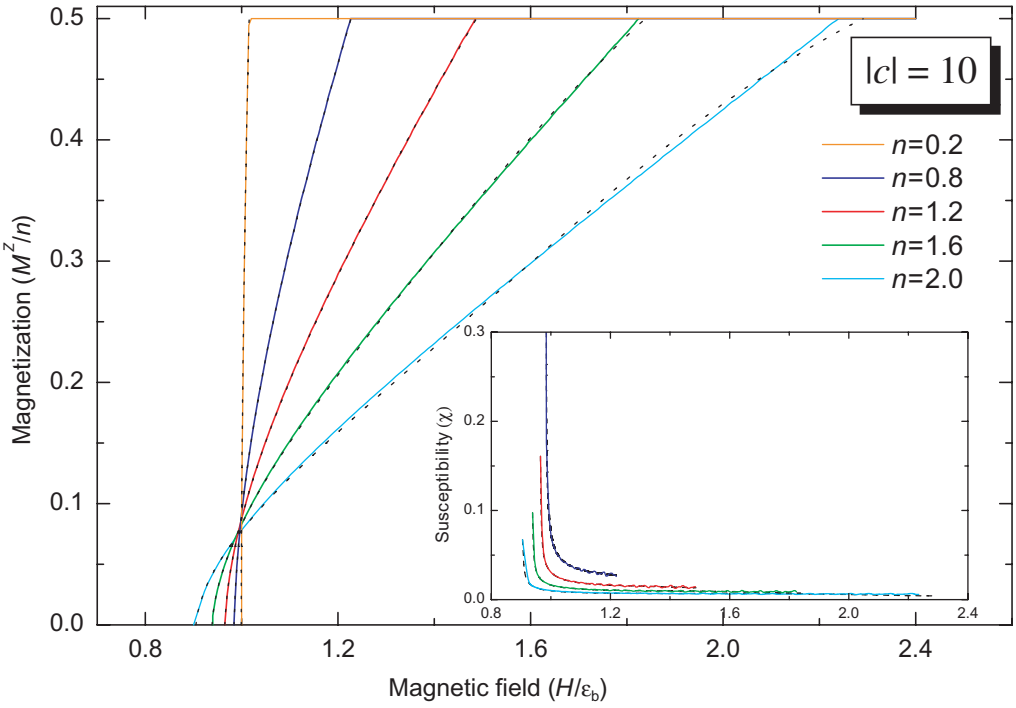

Figure 5. Magnetization M^z/n versus the external field H/ϵ_b for $c = -10$ in the units $2m = \hbar = 1$ for different densities n. The dashed lines are plotted from the analytic result (31). The solid curves are obtained from numerical solutions of the dressed energy equations (8). Excellent agreement is seen between the analytic and numerical results. The inset shows a similar comparison between analytic and numerical results for the susceptibility versus the external field H/ϵ_b.

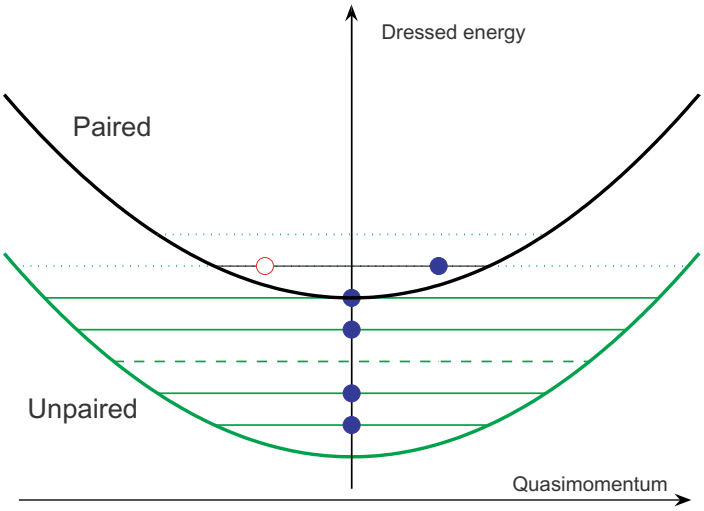

Figure 6. Schematic dressed energy configuration for the gapless phase in the vicinity of H_{c2}.

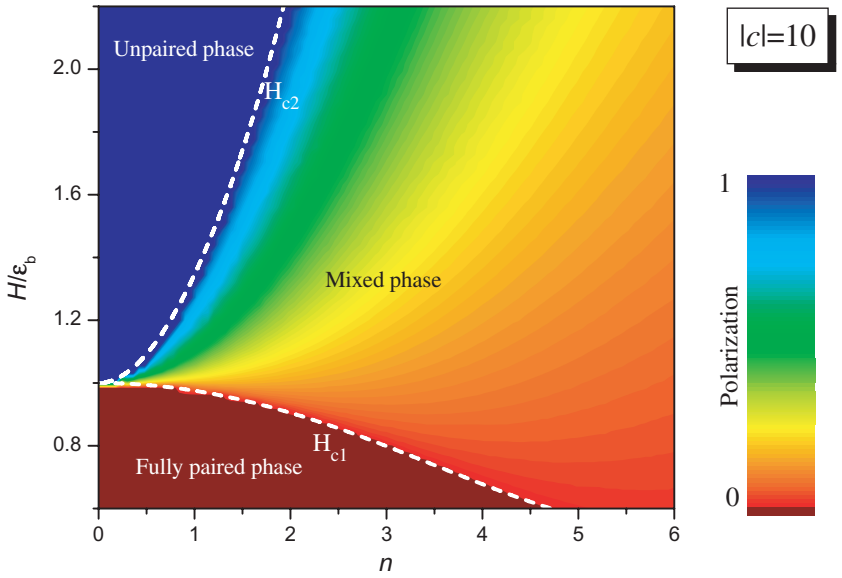

Figure 7. Phase diagram for finite strong interaction with $|c| = 10$. The dashed lines are plotted from equations (28) and (32). The coloured phases are obtained by numerical solution of the dressed energy equations (8). The numerical phase transition boundaries coincide well with the analytic results (28) and (32).

A typical phase diagram in the $n - H$ plane for finite strong interaction is shown in figure 7. Smooth magnetization curves at the critical fields H_{c1} and H_{c2} indicate second-order phase transitions. Very good agreement is observed between the curves obtained from the numerical solution of the dressed energy equations and the analytical predictions (28) and (32) for the critical fields.

7. Conclusion

In summary, we have studied magnetic properties and quantum phase transitions for the 1D BA integrable model of spin-1/2 attractive fermions. The previous work on this model has been extended to derive higher order corrections for the ground-state energy, pressure, chemical potentials, magnetization, susceptibility and critical fields in terms of the external magnetic field, density and interaction strength. The range and applicability of the analytic results have been compared favourably with numerical solutions of the dressed energy equations. The universality class of linear field-dependent behaviour of the phase transitions in the vicinity of the critical field values has been predicted for the whole attractive regime. This universal behaviour is consistent with the prediction for the 1D Hubbard model [59]. However, it appears not to support the argument [45, 46] for a van Hove-type singularity of quantum phase transition for 1D attractive fermions. Finite temperature properties of 1D interacting fermions will be considered elsewhere.

We further confirm that 1D strongly attractive fermions with population imbalance exhibit three quantum phases, subject to the value of the external field H [27]: (i) for $H < H_{c1}$ bound pairs form a singlet ground state, (ii) for $H > H_{c2}$ a completely ferromagnetic phase without pairing occurs, and (iii) for the intermediate range $H_{c1} < H < H_{c2}$ paired and unpaired atoms

coexist. The typical phase diagram is as depicted in figure 7. However, for weak coupling, the BCS-like pairing is unstable. Two quantum phases emerge when the external field is applied: (i) a fully polarized phase for $H > H_c$ and (ii) a coexisting phase of paired and unpaired fermions for $0 < H < H_c$. The phase diagram for weak coupling is illustrated in figure 3. We have shown that the mixed phase in 1D interacting fermions with polarization can be effectively described by two coupled Fermi liquids. Our exact phase diagrams for the weak and strong coupling regimes also provide a space segment signature for an harmonically trapped Fermi gas in 1D geometry. These quantum phases and magnetic properties may also possibly be observed in experiments with ultracold fermionic atoms [60, 61].

Acknowledgments

This work was supported by the Australian Research Council. We thank Miguel Cazalilla, Erhai Zhao and Chaohong Lee for helpful discussions. JSH is supported by the NSFC (no. 10671187), he also thanks the Department of Theoretical Physics, Australian National University for their hospitality during his visit in December 2007. AF thanks CNPq (Conselho Nacional de Desenvolvimento Cientifico e Tecnologico) for financial support. XWG thanks the Department of Mathematics, University of Science and Technology of China and MTB thanks the Centre for Modern Physics, Chongqing University, China for hospitality during various stages of this work.

References

[1] Giorgini S, Pitaevskii L P and Stringari S 2008 *Rev. Mod. Phys.* **80** 1215
Cazalilla M A 2004 *J. Phys. B: At. Mol. Opt. Phys.* **37** S1
Yurovsky V A, Olshanii M and Weiss D S 2008 *Adv. At. Mol. Opt. Phys.* **55** 61
[2] Lewenstein M, Sanpera A, Ahufinger V, Damski B, Sen A and Sen U 2007 *Adv. Phys.* **56** 243
[3] Grimm R 2008 Ultracold Fermi gases *Proc. Int. School of Physics 'Enrico Fermi', Course CLXIV (Varenna, June 2006)* ed M Inguscio, W Ketterle and C Salomon pp 413–62
[4] Ketterle W and Zwierlen M W 2008 Ultracold Fermi gases *Proc. Int. School of Physics 'Enrico Fermi', Course CLXIV (Varenna, June 2006)* ed M Inguscio, W Ketterle and C Salomon pp 95–287
[5] Leggett A J 1980 *Modern Trends in the Theory of Condensed Matter* (Berlin: Springer)
Zwierlein M *et al* 2004 *Phys. Rev. Lett.* **92** 120403
Bourdel T *et al* 2004 *Phys. Rev. Lett.* **93** 050401
[6] Zwierlein M W, Schirotzek A, Schunck C H and Ketterle W 2006 *Science* **311** 492
Zwierlein M W, Schunck C H, Schirotzek A and Ketterle W 2006 *Nature* **442** 54
Shin Y *et al* 2006 *Phys. Rev. Lett.* **97** 030401
[7] Partridge G B *et al* 2006 *Science* **311** 503
Partridge G B *et al* 2006 *Phys. Rev. Lett.* **97** 190407
[8] Schunck C H *et al* 2007 *Science* **316** 867
[9] Chevy F 2006 *Phys. Rev. Lett.* **96** 130401
[10] Chien C C, Chen Q, He Y and Levin K 2007 *Phys. Rev. Lett.* **98** 110404
Stajic J, Chen Q and Levin K 2005 *Phys. Rev. Lett.* **94** 060401
[11] Hu H, Liu X J and Drummond P D 2007 *Phys. Rev. Lett.* **98** 060406
[12] Silva T N D and Mueller E J 2006 *Phys. Rev. Lett.* **97** 070402
Silva T N D and Mueller E J 2006 *Phys. Rev.* A **73** 051602
Haque M and Stoof H T C 2006 *Phys. Rev.* A **74** 011602

[13] Rapp A, Zaránd G, Honerkamp C and Hofstetter W 2007 *Phys. Rev. Lett.* **98** 160405
Honerkamp C and Hofstetter W 2004 *Phys. Rev. Lett.* **92** 170403
[14] Lecheminant P, Boulat E and Azaria P 2005 *Phys. Rev. Lett.* **95** 240402
Capponi S *et al* 2008 *Phys. Rev.* A **77** 013624
[15] Cherng R W, Refael G and Demler E 2007 *Phys. Rev. Lett.* **99** 130406
[16] Wilczek F 2007 *Nat. Phys.* **3** 375
[17] Sarma G 1963 *J. Phys. Chem. Solids* **24** 1029
[18] Fulde P and Ferrell R A 1964 *Phys. Rev.* A **135** 550
Larkin A I and Ovchinnikov Y 1965 *Sov. Phys.—JETP* **20** 762
[19] Liu W V and Wilczek F 2003 *Phys. Rev. Lett.* **90** 047002
[20] Zvonarev M B, Cheianov V V and Giamarchi T 2007 *Phys. Rev. Lett.* **99** 240404
[21] Cazalilla M A and Ho A F 2003 *Phys. Rev. Lett.* **91** 150403
[22] Fuchs J N, Recati A and Zwerger W 2004 *Phys. Rev. Lett.* **95** 090408
Fuchs N, Gangardt D M, Keilmann T and Shlyapnikov G V 2005 *Phys. Rev. Lett.* **95** 150402
[23] Batchelor M T, Bortz M, Guan X W and Oelkers N 2006 *J. Phys. Conf. Ser.* **42** 5
Oelkers N, Batchelor M T, Bortz M and Guan X W 2006 *J. Phys. A: Math. Gen.* **39** 1073
[24] Girardeau M D and Wright E M 2008 *Phys. Rev. Lett.* **100** 200403
[25] Orso G 2007 *Phys. Rev. Lett.* **98** 070402
[26] Hu H, Liu X J and Drummond P 2007 *Phys. Rev. Lett.* **98** 070403
[27] Guan X W, Batchelor M T, Lee C and Bortz M 2007 *Phys. Rev.* B **76** 085120
[28] Feiguin A E and Heidrich-Meisner F 2008 *Phys. Rev.* B **76** 220508
[29] Iida T and Wadati M 2008 *J. Phys. Soc. Japan* **77** 024006
Iida T and Wadati M 2005 *J. Phys. Soc. Japan* **74** 1724
[30] Tezuka M and Ueda M 2008 *Phys. Rev. Lett.* **100** 110403
[31] Batrouni G G, Huntley M H, Rousseau V G and Scalettar R T 2008 *Phys. Rev. Lett.* **100** 116405
[32] Parish M M, Baur S K, Mueller E J and Huse D A 2007 *Phys. Rev. Lett.* **99** 250403
[33] Ying Z J, Cuoco M, Noce C and Zhou H Q 2008 *Phys. Rev. Lett.* **100** 140406
[34] Rizzi M, Polini M, Cazalilla M A, Bakhtiari M R, Tosi M P and Fazio R 2008 *Phys. Rev.* B **77** 245150
[35] Zhao E and Liu W V 2008 *Phys. Rev.* A **78** 063605
[36] Gaudin M 1983 *La fonction d'onde de Bethe* (Paris: Masson)
[37] Schirotzek A, Wu C-H, Sommer A and Zwierlein W 2009 *Phys. Rev. Lett.* **102** 230402
[38] Casula M, Ceperley D M and Mueller E J 2008 *Phys. Rev.* A **78** 033607
[39] Guan L, Chen S, Wang Y P and Ma Z Q 2009 *Phys. Rev. Lett.* **102** 160402
[40] Lüscher A, Noack R M and Läuchi A M 2008 *Phys. Rev.* A **78** 013637
[41] Colomé-Tatché M, Shlyapnikov G V and Tsvelik A M 2007 arXiv:0712.4081
[42] Kakashvili P and Bolech C J 2009 *Phys. Rev.* A **79** 041603
[43] Yang K 2001 *Phys. Rev.* B **63** 140511
[44] Vekua T, Matveeko S I and Shlyapnikov G V 2008 arXiv:0807.4185
[45] Schlottmann P 1997 *Int. J. Mod. Phys.* B **11** 355
[46] Schlottmann P 1994 *J. Phys.: Condens. Matter* **6** 1359
[47] Yang C N 1967 *Phys. Rev. Lett.* **19** 1312
[48] Gaudin M 1967 *Phys. Lett.* A **24** 55
[49] Lieb E and Mattis D 1962 *Phys. Rev.* **125** 164
[50] Giamarchi T 2004 *Quantum Physics in One Dimension* (Oxford: Oxford University Press)
[51] Colomé-Tatché M 2008 arXiv:0801.2640
[52] Guan X W, Batchelor M T and Lee J Y 2008 *Phys. Rev.* A **78** 023621
[53] Takahashi M 1999 *Thermodynamics of One-Dimensional Solvable Models* (Cambridge: Cambridge University Press)

[54] Essler F H L, Frahm H, Göhmann F, Klümper A and Korepin V E 2005 *The One-Dimensional Hubbard Model* (Cambridge: Cambridge University Press)
[55] Batchelor M T, Guan X W, Oelkers N and Tsuboi Z 2007 *Adv. Phys.* **56** 465
[56] Lai C K 1973 *Phys. Rev.* A **8** 2567
[57] Guan X W, Batchelor M T, Lee C and Zhou H Q 2008 *Phys. Rev. Lett.* **100** 200401
[58] Clogston A M 1962 *Phys. Rev. Lett.* **9** 266
[59] Woynarovich F and Penc K 1991 *Z. Phys.* B **85** 269
[60] Stewart J T, Gaebler J P and Jin D S 2008 *Nature* **454** 744
[61] Schunck C H, Shin Y, Schirotzek A and Ketterle W 2008 *Nature* **454** 739